

PERSPECTIVE OPEN ACCESS

Recent Advances in Polyimine Chemistry: Synthesis, Functional Design, and Degradation

Debsena Chakraborty¹ | Alex J. Plajer^{1,2} ¹Macromolecular Chemistry I, Faculty of Natural Science, University of Bayreuth, Bayreuth, Germany | ²Bayrisches Polymer Institut (BPI), Universität Bayreuth, Bayreuth, Germany**Correspondence:** Alex J. Plajer (alex.plajer@uni-bayreuth.de)**Received:** 22 December 2024 | **Revised:** 25 February 2025 | **Accepted:** 25 February 2025**Keywords:** conjugated polymers | degradable polymers | organic semiconductors

ABSTRACT

Polymer materials have come under much scrutiny for the ever-growing amount of plastic waste they generate. Although much recent work focuses on making our current polymer economy more sustainable, efforts to do the same with conjugated polymers are only emerging. This perspective summarizes and contextualizes recent efforts in the synthesis of conjugated polymers, primarily including those with C=N bonds, which have recently garnered attention due to their potential for cleavage. Starting with the exploration of studies that help to understand the underlying chemistry of polyimines, their degradability, and the consequent technological implications are highlighted, which also extend to other cleavage linkers. Furthermore, emerging applications in optoelectronics are highlighted, which make use of the unique chemistry of the imine bond. Our perspective identifies polyimines as an opportunity for a new generation of stimuli-responsive and potentially recyclable and degradable functional materials.

1 | Introduction

The issue of postconsumer plastic waste accumulation has become a significant concern in the eyes of the public, not only because of the ever-growing amount of the very visible waste piles but also because of the dire consequences for both the environment and human health [1]. Traditional petroleum-based plastics featuring all carbon backbones, which are widely used in modern society, persist for centuries after disposal as they show little appreciable degradation with respect to their time in use. While biodegradable polymers featuring links in the polymer main chain that are susceptible to hydrolysis offer some alleviation, there are growing doubts about their ability to degrade effectively in real-world conditions, particularly in marine environments and landfills [2]. Furthermore, giving plastics the label of biodegradability might signal consumers that these can be carelessly disposed of, but as the ecological effects of the degradation products of such novel polymers are often unknown, the uncontrolled release of these must be avoided.

Economically, this also means labor investigated in their synthesis and processing is lost, which is most critical for more intricate polymer structures [3, 4]. An example of these is conjugated polymers, which are an integral part of many advanced semiconductor applications, as these offer a unique combination of desirable optical and electronic properties coupled with the processing advantages of synthetic polymers [5]. Many high-performance applications require highly optimized chemical structures that are accessed by multistep protocols, not only involving precious reactants and catalysts but also consuming an immense amount of time [6]. After device failure, the conjugated polymer is lost when the device is disposed of, with no recycling plan for the conjugated polymer component. In this regard, polymer structures with predetermined breaking points are of interest, as degradability often translates to chemical recyclability into, for example, virgin monomer. This can not only aid in separating components but also help to ultimately obtain materials with properties identical to the original polymer by repolymerization of the

This is an open access article under the terms of the [Creative Commons Attribution](https://creativecommons.org/licenses/by/4.0/) License, which permits use, distribution and reproduction in any medium, provided the original work is properly cited.

© 2025 The Author(s). *Journal of Polymer Science* published by Wiley Periodicals LLC.

recycled monomers [7]. Furthermore, many emerging applications of these organic semiconductors exist at the interface with biology, such as wearable and implantable (bio)electronics and biological sensors [8, 9]. Here, degradability is pivotal to allow for metabolization and excretion of these devices and therapeutics after the treatment. Although there is a clear motivation to develop degradable and recyclable conjugated polymers, the exploration of such remains underexplored. Nevertheless, a number of recent reports showcase the emerging interest in conjugated polymers that allow for degradation while maintaining solubility and thereby processability benefits; these are summarized and contextualized in this perspective. Although by no means exhaustive, we thereby aim to highlight the potential that this emerging class of materials bears. When considering functional groups that feature π -bonds, enabling conjugation with the potential hydrolytic cleavage, the imine bond is a prime candidate. In the following sections, some recent studies are highlighted, which, although not exploring the degradability of the polyimine, still help learn to understand the underlying chemistry and utility of this material class.

2 | General Considerations

Polyimines are often not luminescent due to the existence of various nonradiative decay pathways of excited states, for example, involving E-Z isomerization around the C=N double bond or rotation around the C-N single bond [10]. However, Skene and co-workers reported the trifluoroacetic acid (TFA) catalyzed polycondensation of 9,9'-dialkylated fluorene diamines with 9,9'-dialkylated fluorene dialdehydes, yielding polyimine **1A** (number-averaged molecular weight (M_n) = 9–145 kg/mol by gel permeation chromatography (GPC), polydispersity (D) = 1.3) that showed bright-green luminescence (Figure 1) [11]. An absolute fluorescence quantum yield (Φ_f) of 0.40 was observed in thin films, which was comparable to polyfluorene analogues with an all-C-C polymer backbone. Protonation of the imine lone pair improved quantum yields further, although the reasons for this were unclear. Importantly, when the diamine building block was not alkylated at the 9,9' position of the fluorene, quantum yields were below 0.01, which led the authors to conclude that alkylation suppressed nonradiative decay pathways. Either protonation with TFA or oxidation with FeCl_3 occurred, which could be reverted by neutralization with Et_3N and/or reduction with hydrazine, highlighting the chemical robustness of the imine bond. Electrochemical oxidation at approximately 1.5 V led to a 120 nm bathochromic shift in absorbance, while reduction at -0.2 V regenerated the neutral polymer absorbing at 425 nm.

Relatedly, a 9,9'-dialkylated fluorene bearing both an amino and aldehyde functionality (AB-type monomer) had also been prepared, which underwent self-polycondensation via dehydration with TiCl_4 . This yielded polymers with a degree of polymerization (DP) of 8, with improved quantum yields in solution (0.48 vs. 0.19) compared to the isomer from dialdehyde (AA)-diamine (BB) polycondensation [12]. Surprisingly, now, TFA doping did not enhance but rather quenched the fluorescence, which could be restored upon deprotonation with NEt_3 . Capitalizing on this property, the polymer could then

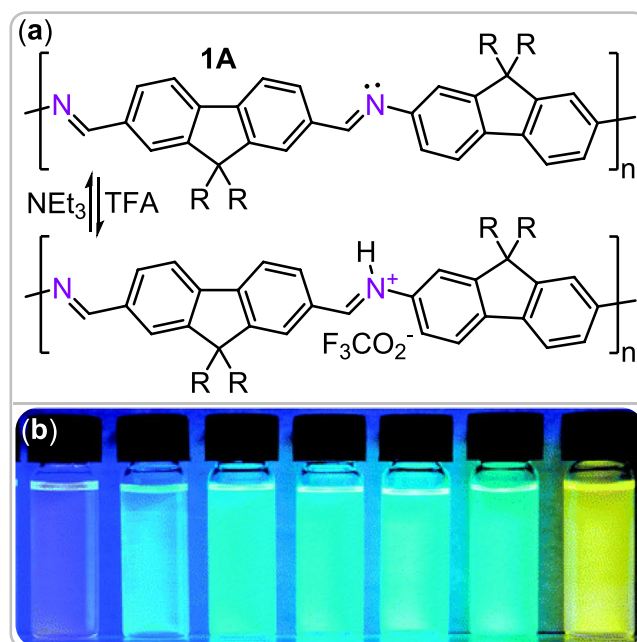


FIGURE 1 | (a) Reversible protonation of the N-lone pair of fluorescent fluorene-based polyimine **1A**. $R = \text{C}_9\text{H}_{19}$. TFA = Trifluoroacetic acid. (b) Fluorescence changes of isomeric fluorene-based polyimine with increasing solvent polarity. Copyright Royal Society of Chemistry 2014 [10].

be used in explosive sensing employing 2,4-dinitrotoluene as a trinitrotoluene (TNT) model. Fluorescence quenching likely involved photoinduced proton transfer from the phenol to the excited imine, with a detection limit of 109 ppm, highlighting the utility of polyimines in sensing applications. Furthermore, this polyimine is solvatochromic [10]. Fluorescence shifted bathochromically by up to 110 nm with increasing solvent polarity, implying that the excited state is more polar than the ground state, which was substantiated by the Lippert–Mataga method. Hence, the polymer could serve as a solvent polarity probe. While the quantum yield was unaffected by residual oxygen for the polymer, it was strongly quenched for the amino-aldehyde AB monomer. Furthermore, moderate fluorescence yields ($\Phi_f \approx 25\%$) were also possible in thin films when co-depositing the polymer in poly(methylmethacrylate).

The portfolio of fluorescent polyimines could also be expanded to a range of copolymers [13]. Both the fluorene-bearing aldehyde or the one bearing imine groups was polycondensed under TFA catalysis with thiophene-containing building blocks bearing the complementary functionality. M_n 's of 6.9–16.4 kg/mol by GPC ($D = 1.2$ – 1.7) were obtained, which according to the authors lay all above the DP at which optoelectronic properties saturate. Φ_f lay around 10%, which again improved upon protonation, and this stood in contrast to the all-thiophene analogue, which was not fluorescent. Notably, the reduction potentials were less affected by the thiophene incorporated into the copolymer than the corresponding oxidation potentials. Yet, the electrochemically generated radical cation could be reduced to restore the original color of the copolymer in spectroelectrochemical studies, demonstrating the robustness of these polyimines. Capitalizing on this property, such polyimines could be used in electrochromic devices

[14]. For this, indium tin oxide-coated glass was spray-coated with a mixture of a diaminothiophene and a triphenylamine dialdehyde. Heating at 120°C for 30 min in an acid-saturated atmosphere induced the rapid formation of the immobilized polyimine. Reversible (electro) chemical switching between its neutral and oxidized states could be achieved without degradation. Hence, transmissive electrochromic devices were engineered that could be cycled between their oxidized (dark blue) and neutral (cyan/light green) states under ambient conditions with applied biases of +3.2 and -1.5 V, respectively.

An all thiophene-imine polymer was synthesized via condensation of the bulk mixed monomers with a weight-averaged molecular weight (M_w) of 15 kg/mol ($D=1.3$) [15]. The imine bond was found stable to even common reducing agents such as NaBH_4 , which usually would reduce imines to amines, and this pointed toward stabilization of the imine group by being embedded in a conjugated motif. This was further evidenced by a quasi-reversible one-electron oxidation peak at 0.54 V that was cathodically shifted compared to a small molecule model. The polymer withstood repeated oxidation and reduction cycles, evidencing high electrochemical stability. The highest occupied molecular orbital (HOMO) and lowest occupied molecular orbital (LUMO) lay at -4.8 and -3.8 eV, respectively, correlating to a band gap of 1.0 eV, which was considerably lower than conventional polythiophenes. Thereafter, these thiophene-based polyimines were employed as the donor material in bulk heterojunction solar cells as the photoactive layer with phenyl- C_{61} -butyric acid methyl ester (PCBM) as the acceptor and showed low power conversion efficiencies of up to 0.22%, which were ascribed to the formation of a coarse morphology [16].

Polycondensation involving aldehyde monomers can result in functional aldehyde chain-ends (Figure 2) [17]. As in-chain imine bonds are stabilized through conjugation toward borane reductants, the aldehyde chain-ends can be selectively functionalized via reductive amination with triacetoxy borohydride reductant while the imine backbone is preserved, as confirmed by GPC for the imine **2A**. With this strategy, molecular weights could also be doubled by coupling two polymer chains through reductive

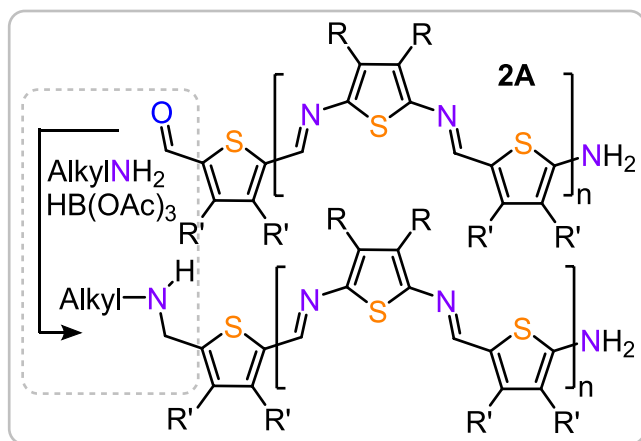


FIGURE 2 | Reductive amination of aldehyde chain-ends of the polyimine **2A** leaves the imine groups intact due to stabilization of these via conjugation.

amination with a diamine. The color of the polyimine could also be tuned by coupling a Dansyl chromophore to the chain-end. Having revealed the reactive nature of the chain ends, it motivated the authors to subject polyimines to the same polycondensation conditions with which they had been generated, resulting in the polymer undergoing further polymerization, almost quintupling its molecular weight from 10 to 47 kg/mol. In the context of the reactivity of the imine bonds it is also worth pointing out that imines feature some dynamicity that can be maintained in these types of materials. In this regard, Hager and co-workers demonstrated thermally triggered imine bond exchange being capable of healing photodamages in thin films of conjugated polyimines [18].

Combined, this section highlights that polyimines exhibit tunable luminescence, electrochemical stability, and dynamic reactivity, enabling applications in sensing, electrochromic devices, and self-healing materials. Alkylation at the fluorene 9,9'-position enhances fluorescence by suppressing nonradiative decay, while protonation and oxidation modulate emission properties. Conjugation stabilizes the imine bond, even against reductants, highlighting their robustness for optoelectronic applications.

3 | Advancing Molecular Design for Optoelectronic Applications

n - π conjugation of the nitrogen lone pair in aromatic imines with the adjacent aromatic ring results in twisted torsion angles disrupting delocalization of the π -system, which is further amplified by the repulsion of the hydrogen atoms. However, the lone pair of the imine group can not only be protonated but also serve as an H-Bond acceptor. Here, Zhang and coworkers recently reported a polyimine **3A** design in which intramolecular hydrogen bonding improved coplanarity to promote π -electron delocalization and intermolecular stacking (Figure 3). This involved an H-bond donating carbamate group, as shown in Figure 3 [19]. Piperazin building blocks between the two imines have also been employed, potentially serving as H-bond acceptor units for the $\text{HC}=\text{N}$ protons. The polymer was accessed via Stille coupling of a dibrominated building block with the preformed H-bond stabilized imines, with a distannylated thiophene-derived building block, yielding copolymers with $M_n = 35$ and 54 (D ca. 2.5). Serving as electron donors with fullerene acceptors in organic solar cells, power conversion efficiencies of up to 10.2% were reached.

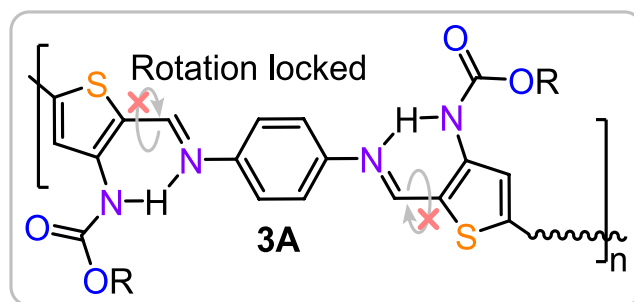


FIGURE 3 | Intramolecular H-Bond strategy restricting rotation around the imine functionality to enhance the planarity of the polymer **3A**. Wavy bond denotes π -conjugated section of the polymer not containing imine bonds.

Further recent attention turned to polymers featuring C=N double bonds in their polymer main chain due to their potential for hydrolysis and other degradation modes. In their initial contribution in 2017, Bao and coworkers prepared a thienodiketopyrrol-based dialdehyde **4A** (Figure 4a) with branched side chains and prepared a polyimine **4B** via polycondensation of phenylene diamine under para-toluenesulfonic acid ($M_n = 40$ kg/mol). Intriguingly, the presence of CaCl_2 as a dehydration agent was crucial to obtain high molecular weights [20]. Adding aqueous acetic acid to an organic polymer solution of **4B** led to substantial breakdown after 3 h and full degradation after 10 h as measured by the decreasing absorption peak associated with the conjugated structure. Degradation also occurred for thin films in acidic buffer, leading to degradation within a month. NMR studies revealed that after imine hydrolysis, further degradation of the diketopyrrol lactam rings occurred, ultimately leading to colorless degradation products. Hole mobilities of $0.34 \text{ cm}^2/\text{Vs}$ were measured in a bottom-gate/top-contact device configuration with gold electrodes. Using cellulose supports and iron electrodes with Al_2O_3 dielectrics, the polymers could then be used in transient electronic devices with hole mobilities of $0.12 \text{ cm}^2/\text{Vs}$ that are stable in neutral water but fully degrade at, for instance, the acidic pH of gastric acid in the human stomach into products that are unlikely to present hazards to either the environment or the human body.

Thereafter the thienodiketopyrrol-based polyimines have been blended with a thermoplastic urethane to obtain a degradable elastomeric material thanks to the polyurethane matrix [22]. The polyimine formed nanoconfined fibers, as shown by atomic force microscopy (AFM) and thereby maintained its semi-conducting properties in the blend. Highly solubilizing side chains had to be installed to avoid micron-sized phase separation, which is undesirable as such domains may localize strain to serve as early points of crack formation. Grazing-incidence small-angle scattering (GIWAXS) showed a fourfold decrease in semiconductor crystallinity upon blending, yet hole mobility was maintained at ca. $0.05 \text{ cm}^2/\text{Vs}$ (compared to $0.14 \text{ cm}^2/\text{Vs}$ of pure polyimine) up to an elastomer content of 70%. The electrical performance was maintained under strain, which is not the case for the pure polyimine without the elastomeric matrix due to the formation of cracks. As both the polyurethane matrix material as well as polyimine are degradable, films of the blend could be degraded in aqueous TFA.

Relatedly, an aldehyde-functionalized dihydropyrrolopyrrole **4C** was copolymerized with phenylene diamine by pTsoH catalysis

and CaCl_2 dehydration ($M_n = 5.4$ kg/mol by NMR end-group analysis) (Figure 4b) [21]. TFA hydrolysis in CDCl_3 of **4D** shows the disappearance of the imine and the evolution of aldehyde resonances after 20 min with no further change after 1 h, which the authors noted to be substantially faster than for other conjugated polyimines. Spin-coated films were afterward subjected to TFA vapor, coloring them bright blue, associated with a bathochromic shift of λ_{max} due to imine protonation, which could be reverted by deprotonation with hydrazine, and this could be reversibly cycled 10 times. As the fluorescence in the polyimine **4D** was quenched through a photoinduced electron transfer mechanism but the parent dihydropyrrolopyrrole monomer **4C** was fluorescent; degradation led to a rapid increase in fluorescence at 525 nm within minutes after the addition of TFA into a CHCl_3 polymer solution (Figure 4c).

While the Schiff base polycondensation approach is attractive from a synthetic point of view, it relies on aldehyde precursors. Because the field of conjugated polymers largely evolved based on cross-coupling reactions, the synthetic library of (even commercially) available building blocks bears functionalities suitable for such reactions. Hence, polyimines from cross-coupling reactions would allow for the easy utilization of such co-monomers. To achieve this, a building block comprising stannylated thiophenes **5B** connected by an imine group could be employed in cross-coupling with a brominated naphthalene diimide **5A**, a popular building block in nondegradable organic semiconductors (Figure 5) [23]. Stille coupling yielded a polyimine **5C** ($M_n = 26$ kg/mol, $D = 1.3$), which, compared to a control polymerization with monomers containing $-\text{C}=\text{C}-$ vinyl rather than $-\text{C}=\text{N}-$ imine groups, even resulted in slightly improved molecular weights. The degradable and

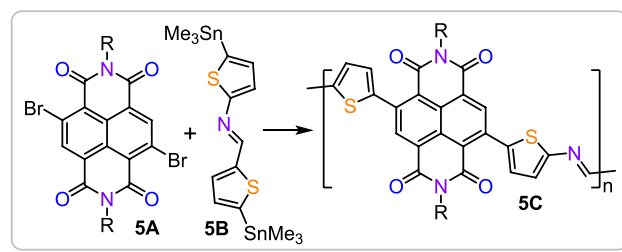


FIGURE 5 | Cross-coupling strategy for naphthalene diimide-derived polyimine **5C** employing a thiophene-containing monomer **5B** with a preformed imine bond.

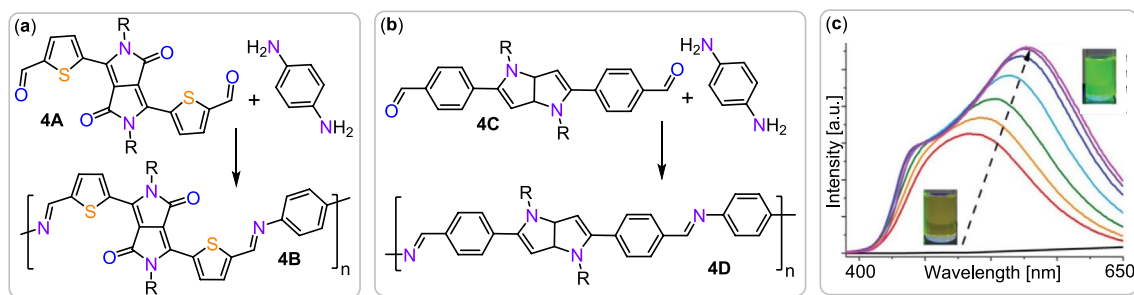


FIGURE 4 | Polycondensation of (a) a diketopyrrol **4A** and (b) a dihydropyrrolopyrrole **4C**-based dialdehyde with phenylene diamine. (c) Acidic degradation of dihydropyrrolopyrrole-derived polymer **4D** produces a fluorescent dialdehyde from a non-emissive polyimine. Copyright Wiley 2023 [21].

nondegradable variants exhibited similar UV-vis spectra with the imine bands hypsochromically shifted. Density functional theory (DFT) revealed a lowered HOMO of the imine relative to the vinyl-containing polymer, which could be experimentally verified by photoemission spectroscopy. Furthermore, the crystalline packing structure is maintained between the vinyl and the imine analogue. Both polymers exhibited ambipolar charge transport in a bottom-gate top-contact field-effect transistor with dominant n-type behavior. Electron saturation mobilities of $0.1 \text{ cm}^2/\text{Vs}$ were obtained for the imine, which is competitive with other naphthalene diimide-based polymers but still reduced compared to the vinyl counterpart ($0.5 \text{ cm}^2/\text{Vs}$). Interestingly, acidic degradation of the naphthalene diimide-based copolymer was faster than for an analogous diketopyrrolopyrrole-derived conjugated imine, which was attributed to the differences in aggregation that the authors explored in more detail thereafter.

For this, brominated thienodiketopyrrolopyrroles with different side chains were Stille coupled with the stannylated dithiophene-imine from before yielding copolymers with $M_n = 16\text{--}33 \text{ kg/mol}$ ($\bar{D} = 2.6\text{--}3.6$, $\text{DP} = 17\text{--}27$) [24]. UV-vis spectroscopy of annealed films examining the vibronic bands revealed that alkyl chain branching close to the chromophore, as well as polymers from terpolymerizations, were associated with weaker interchain aggregation. Photoelectronic spectroscopy showed very similar HOMO and LUMO levels for all polymers, while X-ray diffraction showed the shortest lamellar spacing values and slightly larger $\pi\text{--}\pi$ stacking distances for the side-chain branching point closest to the chromophore. Terpolymers showed a more disordered morphology indicated by their short crystalline coherence length. Saturation Hole mobilities lay between 0.3 and $0.7 \text{ cm}^2/\text{Vs}$, with reduced mobilities for close branching due to weaker interchain $\pi\text{--}\pi$ interactions and shorter order of aggregates. Degradation in chloroform with excess TFA was faster for polymers with the side-chain branching point close to the chromophore and fastest for terpolymers with hydrophilic side chains. Supplying additional water revealed that the degradation rate was very solvent dependent, which is likely caused by aggregation effects in that more pronounced aggregation led to slower hydrolysis. Degradation studies of supported films in aqueous TFA showed similar trends. Hence, factors that enhance the electronic performance ($\pi\text{--}\pi$ stacking distance, crystallite size, and degree of crystallinity) slow down degradation, while increased hydrophilicity that worsens electronic performance due to water traps or ionic impurities enhances degradability.

n-Type semiconductors with a tunable amount of imine bonds were synthesized on a naphthalene diimide basis complementing the many p-type semiconducting polyimines that have been prepared before (Figure 6a) [25]. Randomly terpolymerizing a dibromo naphthalene diimide **6A** with different mixtures of borylated bithiophenes **6B** and **6C** and a phenylene dimine-linked analogue by Suzuki coupling yields a family of terpolymers **6D** with similar weights of $M_n = 50\text{--}65 \text{ kg/mol}$ ($\bar{D} = 2.1\text{--}2.6$) and modular amounts of imine links. Degradation studies in chlorobenzene containing TFA showed that while the polymers without imine links exhibited no degradability, carbonyl NMR resonances emerged for polymers with imine links forming shorter oligomers. Imine

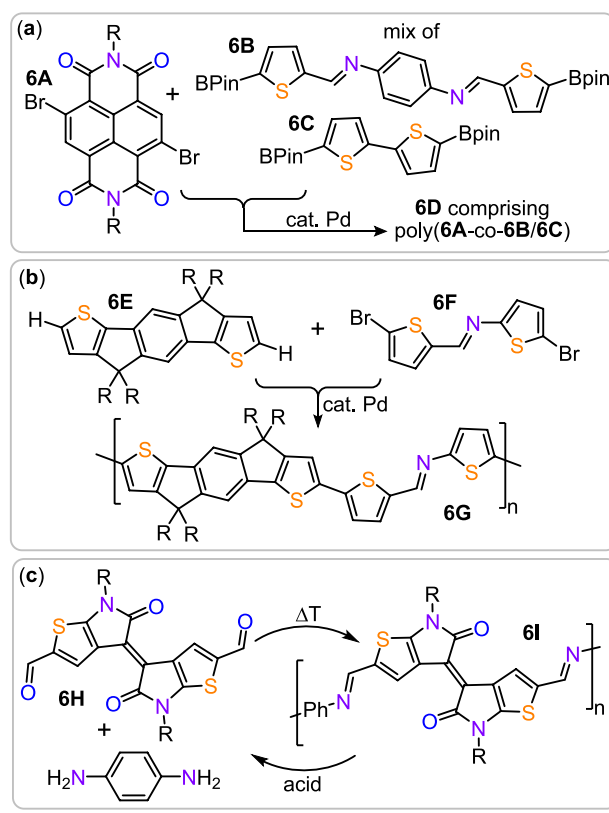


FIGURE 6 | (a) Terpolymerization strategy to tune the imine bond content, combining borylated building blocks **6B** and **6C** with and without imines. (b) Direct arylation strategy to obtain polyimines via CH activation. (c) Chemical recycling recovering pure monomers through hydrolysis.

links were also associated with decreasing electron mobility from $0.23 \text{ cm}^2/\text{Vs}$ without imines to $0.04 \text{ cm}^2/\text{Vs}$ at intermediate amounts to $0.00033 \text{ cm}^2/\text{Vs}$ at the highest amounts of imines investigated. This was rationalized by the imines disturbing the push-pull electronic structure of the imine-free polymer. The authors, however, commented that n-type mobilities reached at intermediate amounts of imines are a sufficient level of performance compared to common n-type semiconductors. Furthermore, higher imine contents were associated with an increasing ratio of edge-on oriented crystallites as well as decreasing $\pi\text{--}\pi$ stacking distances, which helps explain why good electron mobilities were maintained at intermediate imine content. Eventually, a fully disintegrable transistor could be prepared using polyvinylalcohol as the support substrate and dielectric and PEDOT:PSS electrodes in combination with the terpolymer semiconductor. The device completely disintegrated in mixtures of TFA, water, and ethanol at intermediate imine contents.

Moving to other synthetic methodologies, a direct arylation strategy could also be employed to prepare indacenodithiophene-based copolymers **6G** with imine bonds (Figure 6b) [26]. Here, C-H activation of **6E** obviates the necessity for reactive groups on one of the co-monomers in palladium-catalyzed coupling with a second brominated dithiophene building block featuring a preformed imine bond **6F**. Tetramethylethylenediamine, as a coligand, was crucial

to minimize cross-coupling defects, obtaining molecular weights of $M_n = 11\text{--}14\text{ kg/mol}$ ($\mathcal{D} = 1.6\text{--}2.0$). The crude polymers could be further fractionated by washing with hexanes to improve weights to 25 kg/mol . Degradation studies with TFA in chlorobenzene solution showed initial imine protonation indicated by a large bathochromic shift of approximately 200 nm from λ_{max} which was rationalized by favoring the quinoidal resonance form of the polymer. Increasing the acid concentration revealed an isosbestic point, supporting a clean doping process. After initial protonation, degradation of the backbone sets on, leading to imine hydrolysis, which degrades the intense purple-blue polyimine to a faintly yellow solution within days. Unfortunately, no clean process leading to a single degradation product was observed, which would, however, be crucial for chemical recycling. In this process, deconstruction of the polymers would ideally yield one clean product, which could be subject to repolymerization, yielding a polymer with identical properties to the material from a virgin monomer. In this regard, a thioenindigo-based dialdehyde **6H** (Figure 6c) was thereafter polycondensated with para-phenylenediamine or naphthalenediamine under paratoluene sulfonic acid (pTsOH) catalysis and CaCl_2 dehydration to produce chemically recyclable polyimine **6I** ($M_n = 22$ and 19 kg/mol ; $\mathcal{D} = 7$ and 5 after Soxhlet extraction) [27]. Optical band gaps of thin films, as estimated from the onset of absorption, were found to be 1.3 eV , while combined with cyclic voltammetry (CV), a HOMO level at -5.4 and LUMO level at -3.9 eV was estimated. After TFA acid hydrolysis, the UV-vis profiles of the degradation products remained stable for 6 months, indicating that these do not decompose further. Consequently, the starting dialdehyde **6H** could be recovered in $> 90\%$ yield after degradation on a preparative scale, which could then be employed as a monomer to yield materials of similar molecular weights. The polymers exhibited typical p-channel behaviors in organic field-effect transistors (OFETs), as anticipated from the HOMO and LUMO levels, with hole mobilities of $10^{-2}\text{--}10^{-3}\text{ cm}^2/\text{Vs}$, and the polymers from chemically recycled monomer exhibited similar values.

Relatedly, brominated Y5 (a potent electron acceptor unit) derived building block, Stille coupled with a stannylated phenylenebisimine with flanking thiophens to yield the corresponding copolymer ($M_n = 13$, $\mathcal{D} = 1.6$) [28]. TFA-promoted hydrolysis of the polymer produced aldehyde-extended Y5 in 96% yield. This building block could then be repolymerized via imine condensation with phenylene diamine to regenerate the original polymer or produce a network structure with a trifunctional amine. The latter could be used as acceptor polymers in bulk heterojunctions in combination with a conjugated polymer donor that is trapped within the crosslinked imine network, and derived organic photovoltaic (OPV) devices showed photoconversion efficiencies of ca. 13% , which exceed those prepared from Y5 small molecule acceptors. Using the parent copolymer itself as the active layer achieved photoconversion efficiencies of ca. 6% . Organic extraction of the solar cells followed by TFA hydrolysis and filtration over silica gel ultimately yielded the aldehyde-appended Y5 acceptor. Importantly, pure aldehyde was also obtained from the active layer when the photoconversion efficiency decreased after extended light exposure. Hence, the imine hydrolysis sites show potential to be utilized in the recycling of valuable organic electronics even after device failure.

The works highlighted in the section show that molecular design strategies for polyimines in optoelectronics need to balance stability, degradability, and performance. To achieve this synthetically, not only Schiff base polycondensation but also cross-coupling techniques can integrate imine linkages into existing polymer libraries. Intramolecular hydrogen bonding improves coplanarity, promoting π -electron delocalization and intermolecular stacking. Degradation studies reveal a trade-off between electronic performance and stability, where increased π -stacking enhances mobility but slows hydrolysis. Notably, chemically recyclable polyimines allow monomer recovery and repolymerization, paving the way for sustainable organic electronics.

4 | Alternative Building Blocks Enhancing Sustainability and Degradability

However, not performance aspects utilizing optimized building blocks have been in focus, but sustainability concerns using natural product-derived ones. In this regard, a biobased carotene-derived dialdehyde **7A** (Figure 7) was reacted with aromatic diamines under pTsOH catalysis and CaCl_2 dehydration [29]. Bimodal molecular weight distributions were obtained, and the higher weight fraction could be isolated by preparative recycling GPC, yielding a final M_n of 8 kg/mol ($\mathcal{D} = 1.3$). Compared to a model compound, that is, the dialdehyde condensed with 2 equivalents of aniline, λ_{max} shifts from 383 to 470 nm as a consequence of the increased conjugation length. Degradation studies of **7B** revealed an immediate onset of degradation upon HCl addition, observed as a hypsochromically shifted λ_{max} , due to a reduced conjugation length, while NMR studies indicated degradation to the original dialdehyde **7A** and aldehyde-terminated oligomers. Interestingly, exposure to artificial sunlight was found to accelerate acid hydrolysis, while the dialdehyde underwent further photodegradation, photodegrading into epoxides and other aldehyde-containing products. Relatedly, vanillin could be dimerized enzymatically with *Trametes versicolor* to yield a naturally sourced dialdehyde building block for the synthesis of conjugated polyimines [30]. Ethylhexyl chains were installed at the phenol position to improve solubility. Polycondensation with N-alkylated diaminocarbazole or benzene diamine under microwave irradiation yielded copolymers with $M_n = 5\text{--}11\text{ kg/mol}$ ($\mathcal{D} = 1.6$). The carbazole-based main absorption band bathochromically shifted from 364 to 390 nm after polymerization, which was even more amplified in the fluorescence spectra, yet quantum yields were below 2% in solution. Combined, these results

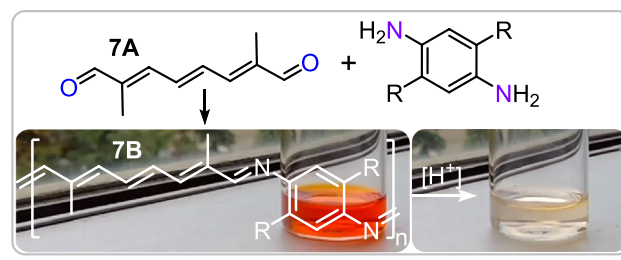


FIGURE 7 | Polycondensation of carotene-derived dialdehyde **7A** and subsequent acidic degradation of the resulting polyimine **7B**. $\text{R} = \text{C}_6\text{H}_{13}$. Copyright American Chemical Society 2023.

suggest that nature's chromophores can be successfully utilized to enhance the sustainability of organic semiconductors.

Taking inspiration from polyimines, efforts have also been made to translate the degradability of the imine bond to conjugated polymers containing heterocyclic building blocks with C=N double bonds within their ring structures. Here, thiophene and imidazole units were alternated via an alkinyl spacer to obtain highly fluorescent and biodegradable conjugated polymer nanoparticles of **8A** (Figure 8a) [31]. Dispersion polymerization via Sonogashira coupling of an alkinyl functionalized thiophene and diiodo *N*-methyl imidazole produced uniform nanoparticles in propanol, a good solvent for the monomers but a bad solvent for the polymer. A surfactant was added to prevent particle aggregation, and molecular weights of ca 15 kg/mol were obtained. Subjecting a fluorescent particle dispersion to aqueous H₂O₂ results in oxidative cleavage of the imidazole groups so that the fluorescence falls linearly to zero. Control particles with oxidatively stable phenylene in place of imidazole linkers did not degrade under the same conditions. Thereafter, the same oxidative degradation could be achieved by macrophages in cell cultures that produce reactive oxygen species (ROS) when exposed to lipopolysaccharides. Cell viabilities between 80% and 100% of macrophages exposed to nanoparticle dispersion showed that the degradation products are nontoxic at low concentrations. Finally, the triple bonds in the polymers could be functionalized via thiol-ene click reactions with cysteine-conjugated folic acid, which was attractive in the context of targeting certain macrophages with folate receptors.

Relatedly, degradable methylimidazol linkers were Sonogashira coupled with extended conjugated building blocks ($M_n = 8$ kg/mol) [32]. The polymer shows aggregation-induced emission and degrades when subjected to H₂O₂ in dimethylformamide/water mixtures to oligomers with $M_n < 1$ kg/mol, which a control polymer without imidazole units did not show. Fluorescence also hypsochromically shifts and decreases upon degradation. The polymer generates ROS under white light irradiation (100 mW/cm²) so that it self-degrades into oligomers. Amides and carboxyl groups were identified as part of the degradation products. Solubilization in aqueous media was achieved by encapsulation of the polymer with pluronic amphiphiles to prepare hydrophilic nanoparticles, which similarly degrade under irradiation but remain stable in the dark. Cell uptake could be tracked with HeLa cells via confocal laser scanning microscopy, thanks to the inherent fluorescence of the encapsulated polymer, and self-degradation upon irradiation could also be confirmed in vitro.

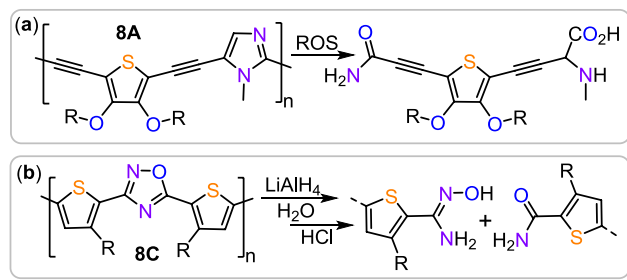


FIGURE 8 | Degradation of (a) imidazole and (b) oxadiazol-based conjugated degradable polymers. ROS, reactive oxygen species.

While the non-irradiated nanoparticles, as well as the degradation products, exhibit excellent cell viability upon irradiation, ROS kill exposed cells, and the degree to which this occurred could be modulated by pre-irradiation of the nanoparticles. This therapy also proved promising in in vivo mouse models following intratumoral injection and white light irradiation, substantially shrinking tumor tissue.

1,2,4-Oxadiazol linkers have also been utilized as degradable linkers that were introduced by a direct arylation strategy to produce a polymer **8C** ($M_n = 4\text{--}5$ kg/mol, $\bar{D} = 1.2\text{--}1.9$) with alternating thiophene units showing photoluminescent quantum yields as high as 40% (Figure 8b) [33]. Small molecule studies revealed the oxadiazol to be stable under strongly acidic or basic conditions, yet reductive cleavage with LiAlH₄ opened the ring to aldimines that were susceptible to acid hydrolysis. Thin film absorption spectra showed prominent vibronic features and the onset of absorbance corresponding to a bandgap of 2.4 eV. Compared to poly(3-hexyl thiophene) (P3HT), that is, the polymer without oxadiazols, this was an increase of the optical bandgap by 0.5 eV. Unfortunately, though the thin film exhibited only partial degradation under conditions where the small molecular model degraded completely, this was ascribed to the low solubility of the polymer. Degradation was evident by some sharp peaks in the ¹H NMR spectrum and a subtle change in the GPC chromatogram at higher molecular weights.

Taken together, heterocyclic C=N-containing conjugated polymers demonstrate promising degradability and functionality, enabling responsive fluorescence, ROS-triggered degradation, and biomedical applications, though solubility and stability remain key challenges for further optimization.

5 | Leveraging the Imine Lone Pair in Metal Coordination

On a different but related note, imine bonds are not only cleavable but also functional due to the coordinating nature of the nitrogen-centered lone pair. Utilizing this feature, transition metal coordination has enabled the application of polyimines in semiconductor applications beyond those explored so far, particularly in the context of electrogenerated light emission. Hence, a dedicated section of this review is devoted to discussing such metallopolymers. Polyimines designed for metal coordination differ from the other polyimines discussed so far in one central aspect: they possess an additional donating atom, here a pyridine nitrogen, in close proximity to the imine nitrogen. This arrangement enables the two donating atoms to function as a chelating group, facilitating the binding of metal ions or metal complex fragments. In 2011, Nitschke and colleagues introduced a novel class of polyimine-based metallopolymers (**9A**, Figure 9a) [34]. Their synthesis involved reacting 1,4-diaminobenzene and 4,4'-diformyl-3,3'-bipyridine in the presence of Cu(I) salts of weakly coordinating tetrafluoroborate counterion and trioctylphosphine. End-group analysis of **9A** by ¹H NMR spectroscopy revealed a number-averaged DP of eight, corresponding to a molecular weight of approximately 9 kg/mol. Intriguingly, the polymer displayed a temperature-dependent sol-gel transition. Solutions within a 2.0–0.7 wt% concentration range formed gels at temperatures of around 130°C. This phase

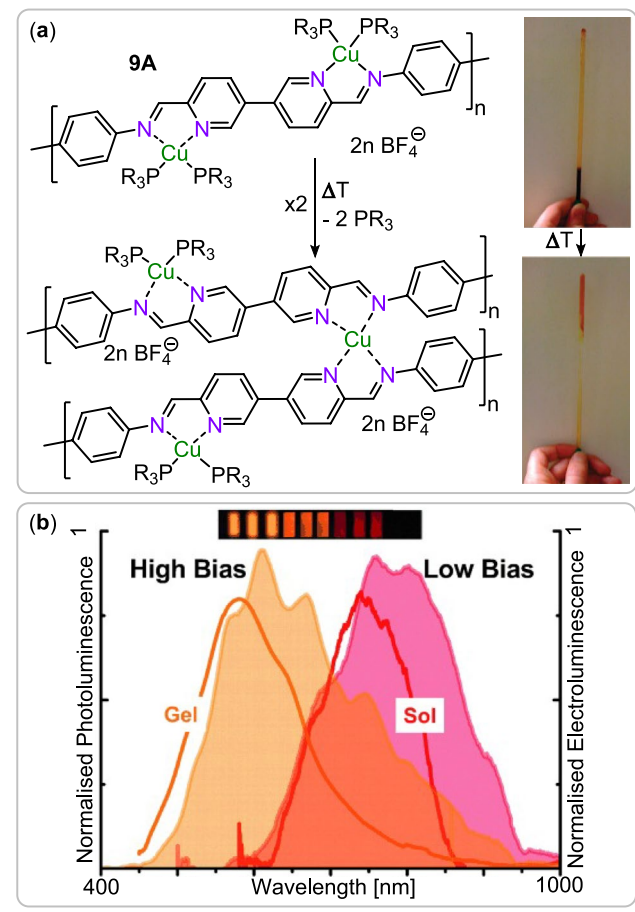


FIGURE 9 | (a) Reversible temperature-triggered sol-gel transition of the polyimine metallo-polymer **9A**. $R = C_8H_{17}$. Copyright 2011 American Chemical Society [34]. (b) Electroluminescence and photoluminescence spectra of the related polymer at different biases and temperatures, respectively. Copyright 2014 WILEY-VCH Verlag GmbH & Co. KGaA [35].

transition was attributed to the formation of $[CuN_4]^+$ complexes resulting in thermally reversible cross-linking and hence gelation, underscoring the potential utility of these metallo-polymers as stimuli-responsive materials.

Enhancing electrooptical properties, an analogous metallo-polymer was prepared with bis[2-(diphenylphosphino)phenyl]ether in place of trioctylphosphine coligands [35]. NMR end group analysis indicated a DP of around seven repeating units, consistent with diffusion-ordered spectroscopy (DOSY) results, suggesting a number average molecular weight of 12 kg/mol. The polymer exhibited photoluminescence (PL) with a maximum (λ_{max}) at 780 nm, attributed to the metal-to-ligand-charge transfer (MLCT) transition. Heating a 1 wt.% polymer solution above 160°C triggered a phase transition to an opaque yellow gel with a significantly hypsochromically shifted emission maximum (λ_{max}) at 580 nm. At elevated temperatures, the $[Cu(POP)]^+$ complex fragment dissociates from the polymer backbone, again leading to gelation. The loss of Cu-N bonds results in the quenching of MLCT-based PL, and hypsochromically shifted emission from the free polyimine was observed. These findings led to the fabrication of light-emitting electrochemical cell (LEC) devices using this polymer, which demonstrated a similar

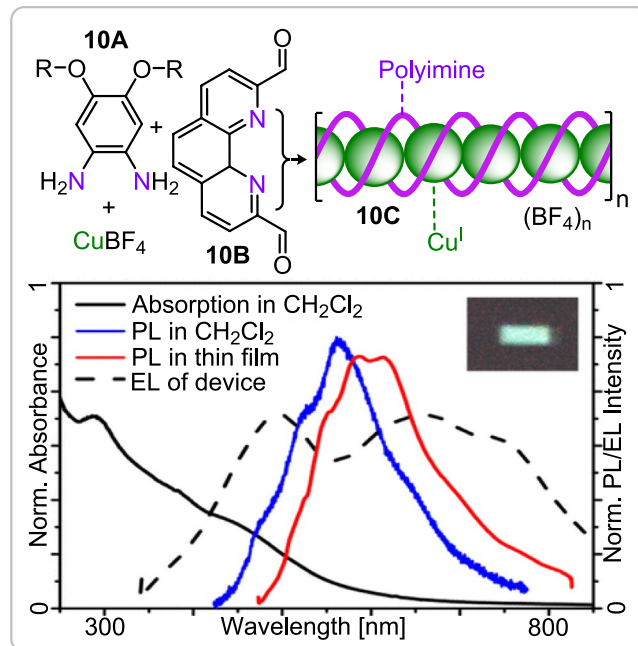


FIGURE 10 | Formation of polyimine helical metallo-polymer **10C** alongside absorption, electroluminescence (EL), and PL spectra of the polymer. $R =$ oligoethyleneglycol Copyright 2012 American Chemical Society [36].

color transition in the electroluminescence spectra. At low bias, the electroluminescence spectra closely resembled the PL spectra of the polymer solutions at low temperature, while at high bias, luminescence aligned well with the spectra of the thermally generated gel (Figure 9b).

Employing diamine **10A** and dialdehyde **10B** with angle rather than linear orientation of the functional groups, in copper-templated polycondensation without additional co-ligands, allows the construction of helical polymer **10C** (Figure 10) [36]. The resulting polymeric structure stabilized the central Cu(I) chain against oxidative decomposition. The polymer exhibited a half-wave potential ($E_{1/2}$) of 0.52 V and a HOMO-LUMO band gap of 2.14 eV. Due to its MLCT states, the polymer displayed broad emission (450–750 nm) centered around 562 nm. Leveraging its broad emission, favorable redox potentials, and band gap, this polymer was successfully employed in the fabrication of white light-emitting LECs.

Similar helical metallo-polymers (averaging 75 repeat units, 28 kg/mol) were then prepared through the imine self-condensation of a building block bearing both imine and aldehyde functionalities in the presence of copper(I)triflimide [37]. Notably, this synthetic approach enabled precise control over polymer length by introducing amine and aldehyde capping agents. UV-vis spectroscopy revealed a bathochromic shift in the $\pi-\pi^*$ absorption band of the polymer with increasing monomer to end-group ratio, indicative of increasing conjugation, which was further reflected in the emission spectra. The color of emitted light shifted from blue-white for shorter oligomers to yellow-white for longer polymers. Interestingly, chirality in these helical polymers could be induced using chiral monomers, chiral solvent, or a chiral initiator [38]. For example,

self-condensation with enantiopure 1-(naphthalen-1-yl)ethan-1-amine as a capping agent formed a helical polyimine polymer with controlled handedness and an average length of 50 repeat units. Thin films of this polymer exhibited a high aspect ratio, with rod-like structures measuring tens of nanometers in length and averaging 10 nm in width. Investigating the electrical properties revealed that the polymers could be rendered conductive via oxidation induced by an external electric field [39]. Furthermore, the oxidation of Cu(I) to Cu(II) caused a Jahn-Teller distortion in the metal ions, resulting in the compression of the overall structure. These examples nicely showcase the transformative power of metal coordination in polyimine systems, allowing these polymers to dynamically adjust their physical properties in response to external stimuli.

Metal-coordination extends the functionality of degradable conjugated polyimines, enabling tunable sol-gel transitions, electroluminescence, and chiral architectures, with potential applications in stimuli-responsive optoelectronics.

6 | Conclusions and Outlook

Looking at the combined advances presented in this contribution, the notion emerges that structural design concepts exist to maintain functionality while enabling degradability in conjugated polymers, focusing on C=N double bonds as either imines or N-heterocycles. Although electro-optical performance can worsen compared to materials comprising a carbon backbone, sufficient performance can be maintained for device applications and enhanced via metal coordination. Also, material characteristics such as strong interactions between polymer chains, which are favorably associated, for example, with charge carrier mobility, hinder degradability. Clearly, one of the challenges is balancing degradability with material performance. Here, one must wonder what density of degradation sites and sensitivity of those to degradation are necessary. It might not be necessary for each and every application that a conjugated polymer can be degraded under the mildest conditions, and a more tailored approach could be appropriate. Particularly, chemical polymer-to-monomer recycling is also a viable end-of-use option for these materials under harsher conditions employing more specialized reagents. In this regard, methodology development could focus on breaking some of the more labile carbon-carbon bonds in conjugated wastes to extract potential monomers. Furthermore, a few breaking points can be sufficient to enable chemical recyclability, and this strategy would be most powerful in combination with breaking points that only cleave under very specific conditions when needed. This could be more in focus in the future to still benefit from the impressive developments of high-performing organic electronic building blocks while introducing the possibility of chemical recyclability. Regarding recyclability, the field currently lacks detailed quantification. To strengthen the discussion and improve the comparability of different materials, it is essential to provide concrete data on monomer recovery percentages following depolymerization, as well as information on the number of times these materials or devices can be effectively recycled without deterioration of performance. Furthermore, unlike non-conjugated polymers such as polyesters or polycarbonates, which are investigated in the context of chemical recycling, many polyimines discussed

in this perspective contain extensive conjugated systems prone to oxidative degradation. This must be considered when designing chemical recycling processes to ensure the recovery of high-purity monomers. From a practical perspective, the cost of the monomers must also be considered, as the materials presented in this perspective are largely produced through expensive synthetic strategies that limit their industrial relevance. Furthermore, the effect of the imine bond on long-term stability should be investigated in future studies, as device lifetime is already a limiting factor in many commercial applications of organic semiconductors. Incorporating sensitive bonds into the material may exacerbate this issue. While the environmental impact of degradation products also warrants future investigation, particularly since hydrolysis combined with oxidation can introduce water-solubilizing groups into the building blocks, the relatively small quantities of materials being considered, compared to those investigated to replace current structural commodity polymers, may make these investigations less critical. Nevertheless, there also remains a need for more labile polymer structures that do not rely on specialty reagents or harsher conditions for deconstruction, so these even fall apart under biological conditions. As seen in this perspective, these properties can be important in the context of self-degradable therapeutics or fully disintegrable electronics. For both cases, the move to more hydrophilic materials to promote water diffusion could be interesting, and in this regard, conjugated polyelectrolytes with cleavable bonds could, for example, be investigated. Particularly in the latter case, though, a less linear and more sudden degradation profile might be desirable so that, for example, an implanted device remains fully functional, resisting degradation until a certain point when degradation becomes rapid, making performance more reliable up until degradation. Again, the design of new polymer structures could solve this problem by combining different reactivities. One concept could involve the slow reaction of certain appended functional groups, which could, for example, turn the polymer more hydrophilic and trigger the hydrolysis of labile links in the polymer backbone. Another concept concerns core-shell structures involving a core (a slower-degrading material) that can be encapsulated by a shell (a faster-degrading material) so when the shell starts degrading, it exposes the core to the environmental conditions, leading to rapid breakdown of the entire structure. Alternatively, self-amplifying degradation could be of interest involving structures that upon degradation release other agents (e.g., small molecules, free radicals, or ions) that further accelerate the degradation process. Lastly, the C=N double bond should not only be viewed as a breaking point but also as a binding site that can enhance and tailor material performances via, for example, coordination to the nitrogen-centered lone pair while maintaining the dynamicity of the imine double bond. Here, the plethora of imine-based ligand scaffolds remains underutilized and hence to be explored to combine functionality with dynamicity [40]. Taken together, the development of ever more tailored polymer structures hence promises not only to drive future technological advances but also to make these, as well as old technologies, more sustainable.

Conflicts of Interest

The authors declare no conflicts of interest.

References

1. M. Subramanian, "Plastics Tsunami: Can a Landmark Treaty Stop Waste From Choking the Oceans?," *Nature* 611 (2022): 650–653.
2. T. P. Haider, C. Völker, J. Kramm, K. Landfester, and F. R. Wurm, "Plastics of the Future? The Impact of Biodegradable Polymers on the Environment and on Society," *Angewandte Chemie, International Edition* 58 (2019): 50–62.
3. A. Rahimi and J. M. García, "Chemical Recycling of Waste Plastics for New Materials Production," *Nature Reviews Chemistry* 1 (2017): 1–11.
4. G. W. Coates and Y. D. Y. L. Getzler, "Chemical Recycling to Monomer for an Ideal, Circular Polymer Economy," *Nature Reviews Materials* 5 (2020): 501–516.
5. A. Köhler and H. Bässler, *Electronic Processes in Organic Semiconductors: An Introduction* (John Wiley & Sons, 2015).
6. K. Müllen and U. Scherf, "Conjugated Polymers: Where we Come From, Where we Stand, and Where we Might Go," *Macromolecular Chemistry and Physics* 224 (2023): 2200337.
7. M. Häußler, M. Eck, D. Rothauer, and S. Mecking, "Closed-Loop Recycling of Polyethylene-Like Materials," *Nature* 590, no. 7846 (2021): 423–427, <https://doi.org/10.1038/s41586-020-03149-9>.
8. A. Chortos, J. Liu, and Z. Bao, "Pursuing Prosthetic Electronic Skin," *Nature Materials* 15, no. 9 (2016): 937–950, <https://doi.org/10.1038/nmat4671>.
9. N. Matsuhsa, X. Chen, Z. Bao, and T. Someya, "Materials and Structural Designs of Stretchable Conductors," *Chemical Society Reviews* 48 (2019): 2946–2966.
10. C. Mallet, A. Bolduc, S. Bishop, Y. Gautier, and W. G. Skene, "Unusually High Fluorescence Quantum Yield of a Homopolyfluorenylazomethine – Towards a Universal Fluorophore," *Physical Chemistry Chemical Physics* 16 (2014): 24382–24390.
11. S. Barik and W. G. Skene, "A Fluorescent All-Fluorene Polyazomethine—Towards Soluble Conjugated Polymers Exhibiting High Fluorescence and Electrochromic Properties," *Polymer Chemistry* 2 (2011): 1091–1097.
12. C. Mallet, M. L. Borgne, M. Starck, and W. G. Skene, "Unparalleled Fluorescence of a Polyazomethine Prepared From the Self-Condensation of an Automer and Its Potential Use as a Fluorimetric Sensor for Explosive Detection," *Polymer Chemistry* 4 (2013): 250–254.
13. S. Barik, T. Bletzacker, and W. G. Skene, " π -Conjugated Fluorescent Azomethine Copolymers: Opto-Electronic, Halochromic, and Doping Properties," *Macromolecules* 45 (2012): 1165–1173.
14. L. Sicard, D. Navarathne, T. Skalski, and W. G. Skene, "On-Substrate Preparation of an Electroactive Conjugated Polyazomethine From Solution-Processable Monomers and Its Application in Electrochromic Devices," *Advanced Functional Materials* 23 (2013): 3549–3559.
15. M. Bourgeaux and W. G. Skene, "A Highly Conjugated p- and n-Type Polythiophenoazomethine: Synthesis, Spectroscopic, and Electrochemical Investigation," *Macromolecules* 40 (2007): 1792–1795.
16. A. Bolduc, S. Barik, M. R. Lenze, K. Meerholz, and W. G. Skene, "Polythiophenoazomethines – Alternate Photoactive Materials for Organic Photovoltaics," *Journal of Materials Chemistry A* 2 (2014): 15620–15626.
17. S. Barik and W. G. Skene, "Selective Chain-End Postpolymerization Reactions and Property Tuning of a Highly Conjugated and all-Thiophene Polyazomethine," *Macromolecules* 43 (2010): 10435–10441.
18. J. Ahner, M. Micheel, R. Geitner, et al., "Self-Healing Functional Polymers: Optical Property Recovery of Conjugated Polymer Films by Uncatalyzed Imine Metathesis," *Macromolecules* 50 (2017): 3789–3795.
19. B. Zhang, Y. Wang, K. Lin, Y. Zhou, and Q. Zhang, "Hydrogen-Bonded Polyazomethines for Efficient Organic Solar Cells," *Journal of Materials Chemistry C* 12 (2024): 2016–2024.
20. T. Lei, M. Guan, J. Liu, et al., "Biocompatible and Totally Disintegrable Semiconducting Polymer for Ultrathin and Ultralightweight Transient Electronics," *Proceedings of the National Academy of Sciences* 114 (2017): 5107–5112.
21. K. A. Bartlett, A. Charland-Martin, J. Lawton, A. L. Tomlinson, and G. S. Collier, "Azomethine-Containing Pyrrolo [3, 2-b] Pyrrole Copolymers for Simple and Degradable Conjugated Polymers," *Macromolecular Rapid Communications* 45 (2024): 2300220.
22. H. Tran, V. R. Feig, K. Liu, et al., "Stretchable and Fully Degradable Semiconductors for Transient Electronics," *ACS Central Science* 5 (2019): 1884–1891.
23. H. Tran, S. Nikzad, J. A. Chiong, et al., "Modular Synthesis of Fully Degradable Imine-Based Semiconducting p-Type and n-Type Polymers," *Chemistry of Materials* 33 (2021): 7465–7474.
24. J. A. Chiong, Y. Zheng, S. Zhang, et al., "Impact of Molecular Design on Degradation Lifetimes of Degradable Imine-Based Semiconducting Polymers," *Journal of the American Chemical Society* 144 (2022): 3717–3726.
25. H. Park, Y. Kim, D. Kim, S. Lee, F. S. Kim, and B. J. Kim, "Disintegrable N-Type Electroactive Terpolymers for High-Performance, Transient Organic Electronics," *Advanced Functional Materials* 32 (2022): 2106977.
26. N. S. Y. Hsu, A. Lin, A. Uva, S. H. Huang, and H. Tran, "Direct Arylation Polymerization of Degradable Imine-Based Conjugated Polymers," *Macromolecules* 56 (2023): 8947–8955.
27. N. Nozaki, A. Uva, H. Matsumoto, H. Tran, and M. Ashisawa, "Thienoisindigo-Based Recyclable Conjugated Polymers for Organic Electronics," *RSC Applied Polymers* 2 (2024): 163–171.
28. H. Jin, K. Kim, S. Park, et al., "Chemically Recyclable Conjugated Polymer and One-Shot Preparation of Thermally Stable and Efficient Bulk-Heterojunction From Recycled Monomer," *Advanced Functional Materials* 33 (2023): 2304930.
29. A. Uva, A. Lin, and H. Tran, "Biobased, Degradable, and Conjugated Poly(Azomethine)s," *Journal of the American Chemical Society* 145 (2023): 3606–3614.
30. G. Garbay, L. Giraud, S. M. Gali, et al., "Divanillin-Based Polyazomethines: Toward Biobased and Metal-Free π -Conjugated Polymers," *ACS Omega* 5 (2020): 5176–5181.
31. T. Repenko, A. Rix, S. Ludwanowski, et al., "Bio-Degradable Highly Fluorescent Conjugated Polymer Nanoparticles for Bio-Medical Imaging Applications," *Nature Communications* 8 (2017): 470.
32. H. Huang, W. Xie, Q. Wan, et al., "A Self-Degradable Conjugated Polymer for Photodynamic Therapy With Reliable Postoperative Safety," *Advancement of Science* 9 (2022): 2104101.
33. B. R. Varju and D. S. Seferos, "Direct Heteroarylation Polymerization of a π -Conjugated Polymer With Degradable 1,2,4-Oxadiazole Linkers," *Polymer Chemistry* 13 (2022): 6386–6392.
34. X. de Hatten, N. Bell, N. Yufa, G. Christmann, and J. R. Nitschke, "A Dynamic Covalent, Luminescent Metallopolymer That Undergoes sol-To-Gel Transition on Temperature Rise," *Journal of the American Chemical Society* 133 (2011): 3158–3164.
35. D. Asil, J. A. Foster, A. Patra, et al., "Temperature- and Voltage-Induced Ligand Rearrangement of a Dynamic Electroluminescent Metallopolymer," *Angewandte Chemie, International Edition* 53 (2014): 8388–8391.
36. X. de Hatten, D. Asil, R. H. Friend, and J. R. Nitschke, "Aqueous Self-Assembly of an Electroluminescent Double-Helical Metallopolymer," *Journal of the American Chemical Society* 134 (2012): 19170–19178.
37. J. L. Greenfield, F. J. Riszuto, I. Goldberga, and J. R. Nitschke, "Self-Assembly of Conjugated Metallopolymers With Tunable Length and Controlled Regiochemistry," *Angewandte Chemie, International Edition* 56 (2017): 7541–7545.

38. J. L. Greenfield, E. W. Evans, D. Di Nuzzo, M. Di Antonio, R. H. Friend, and J. R. Nitschke, "Unraveling Mechanisms of Chiral Induction in Double-Helical Metallopolymers," *Journal of the American Chemical Society* 140 (2018): 10344–10353.
39. J. L. Greenfield, D. Di Nuzzo, E. W. Evans, et al., "Electrically Induced Mixed Valence Increases the Conductivity of Copper Helical Metallopolymers," *Advanced Materials* 33 (2021): 2100403.
40. M. Oh and C. A. Mirkin, "Chemically Tailorable Colloidal Particles From Infinite Coordination Polymers," *Nature* 438 (2005): 651–654.